Vibrational Investigation And Potential Energy Surface Scan Analysis Of NLO Chromophore 4-Dimethyl Aminobenzoic Acid Ethyl Ester

D. Jaya Reshmi, D. Arul Dhas

Abstract: The present study aims to provide deeper knowledge about the structural activity, spectroscopic analysis and nonlinear optical activity of 4-dimethyl aminobenzoic acid ethyl ester (compound 1). The related compound, 2-hydroxy ethyl 4-dimethyl amino benzoate (compound 2) was also calculated with the aid of computational methods. The geometry optimization has been performed to analyze the NLO active site with bonding features of the three compounds by DFT/6-311G (d, p) level. Nature of the hydrogen bonds, intramolecular charge transfer interactions, hyperconjugative interaction and charge delocalization were characterized by NBO analysis. The HOMO and LUMO energies were calculated inorder to check the chemical stability of the molecules. Molecular electrostatic potential (MESP) image illustrate the charge distributions to scrutinize the nonlinear optical active area. The stable conformer of compound had been identified by potential energy surface scan (PES) analysis, which leads to the NLO activity. The dipole moment, polarizability and first, second order hyperpolarizabilities of the title molecule were calculated. The energy gap between frontier orbitals has been used along with electric moments and first order hyperpolarizability to understand the non-linear optical (NLO) activity of the compound. The NLO activity of compound 1 was confirmed by SHG analysis.

Keywords: DFT, MESP, NLO, SHG

1 INTRODUCTION

Benzoic acid and its derivatives are good inhibitors of influenza viruses. Several benzoic acid derivatives such as 4-aminobenzoic acid have been reported in coordination chemistry as bifunctional organic ligands due to their coordination modes. The structural geometry and vibrational spectra of 4-Dimethyl aminobenzoic acid ethyl ester (compound 1) using theoretical and experimental technique have been analyzed and compared with compound 2. 4-Dimethyl aminobenzoic acid ethyl ester is a photo initiator in visible light system and it can be used as a photo initiator in cell encapsulation applications [1]. The generic name of compound 1 is Parbenate. The molecular formula for compound 1 is $C_{11}H_{15}NO_2$. It is a white crystalline powder soluble in organic solvents such as ethanol and acetone. A systematic study on the optimized parameters of the molecules and a detailed vibrational analysis based on FT-IR and FT-Raman spectra is undertaken. HOMO, LUMO analysis, natural charge analysis and redistribution of electron density (ED) in various bonding and anti-bonding orbitals had been calculated by natural bond orbital (NBO) analysis. The dipole moment, nonlinear optical properties (NLO), first, second and third order non-linear hyper polarizabilities have also been studied. The second harmonic generation has been measured using Kurtz-perry technique.

- *D. Jaya Reshmi, D. Arul Dhas*
- *Research Scholar, Register Number: 11975, Department of Physics & Research Centre, Nesamony Memorial Christian College Marthandam – 629165. Affiliated to Manonmaniam Sundaranar University, Abishekapatti, Tirunelveli – 627012, Tamil Nadu, India. rajreshmidev@gmail.com*
- *Associate Professor, Department of Physics & Research Centre, Nesamony Memorial Christian College Marthandam – 629165. Affiliated to Manonmaniam Sundaranar University, Abishekapatti, Tirunelveli – 627012, Tamil Nadu, India. aruldhas2k4@gmail.com*

2. EXPERIMENTAL DETAILS

The compound under investigation 4-Dimethyl aminobenzoic acid ethyl ester (compound 1) is purchased from Sigma Aldrich chemicals (USA) with a stated purity of 99% and used as such for the spectral measurements. The Fourier transform infrared spectrum of the title compound was investigated at room temperature and it was recorded in the range between 400 - 4000 cm^{-1} with a BRUKER IFS 66V model spectrometer equipped with an MCT detector, a KBr beam splitter and globar arc source. The FT-Raman spectrum of compound 1 was recorded on a computer interfaced BRUKER IFS 66V model interferometer equipped with FRA-106 FT Raman accessories. The second harmonic generation behavior was assessed by Kurtz powder technique.

3. COMPUTATIONAL DETAILS

In the present study, all geometrical parameters for the three compounds were optimized by DFT/B3LYP level theory using the 6-311G (d, p) basis set. The optimized geometrical parameters and fundamental vibrational frequencies are calculated theoretically using Gaussian 09 W software. The theoretical results have enabled us to make the detailed assignments of the experimental IR and Raman spectra of the molecule. Chemcraft program was utilized to draw the structure of the optimized geometry and to visualize the HOMO, LUMO pictures. Vibrational mode assignments were made by visual probing of the modes animated using Gauss View program [2]. Natural bond orbital (NBO) and natural population analysis (NPA) were performed using NBO 5.0 program [3]. MESP, PES and second order hyperpolarizability calculation was done by DFT method.

4. RESULT AND DISCUSSION

4.1 Optimized geometry

Fig. 1 shows the optimized molecular structures of compounds 1 and 2 calculated at B3LYP/6-311G (d,p) level basis set and the optimized molecular parameters are listed in table 1. For compounds 1 and 2 the experimental and theoretical data shows that the C-C bond lengths are observed in the range

1.371-1.411 Å and 1.382-1.416 Å respectively. In the ring, the low bond distance measured at C_1-C_2 is 1.371Å denotes the C_2-H_8 …O_{21} inter-molecular hydrogen bonding and C_4-C_5 is 1.384Å indicating C_4-H_9…O_{22} inter-molecular hydrogen bonding. Due to the substitution of dimethyl amino group in the place of hydrogen atom in benzene ring, the bond length of C_2-C_3 is 1.389Å and C_3-C_4 bond length is 1.395Å. The electronegative oxygen atom affects the bond C_{23}-C_{26}, so it has high value of 1.492 Å. Theoretical values for C_{20}=O_{21} are 1.209 Å and 1.211 Å respectively. DFT calculation indicates an increase in the exocyclic angles C_1-C_6-N_{11} and C_5-C_6-N_{11} and the reduction in the endocyclic angle C_1-C_6-C_5 which is due to charge-transfer interaction in D-π-A molecules [4, 5]. The existence of two methyl groups provide the additional negative charges to the amino nitrogen atom resulting in the contraction of C_6-N_{11} bond length. Both endocyclic and exocyclic bond angles show the non-aromatic character. The endocyclic bond angles C_1-C_5-C_6, C_1-C_2-C_3, C_4-C_5-C_6, C_2-C_3-C_4 and C_3-C_4-C_5 are 116.74˚, 121.7˚, 121.2˚, 117.4˚ and 121.6˚. The exo-cyclic bond angles C_3-C_{20}=O_{21}, C_{21}=C_{20}-O_{22}, C_5-C_6-N_{11}, C_1-C_6-N_{11} and C_3-C_{20}-O_{22} are 124.59˚, 123.01˚, 121.7˚, 121.5˚ and 112.40˚ respectively, which shows non-aromatic character. The dihedral angles C_1-C_6-N_{11}-C_{12} and C_2-C_3-C_{20}-O_{21} show that the dimethyl amino group is essentially nonplanar with the benzene ring.

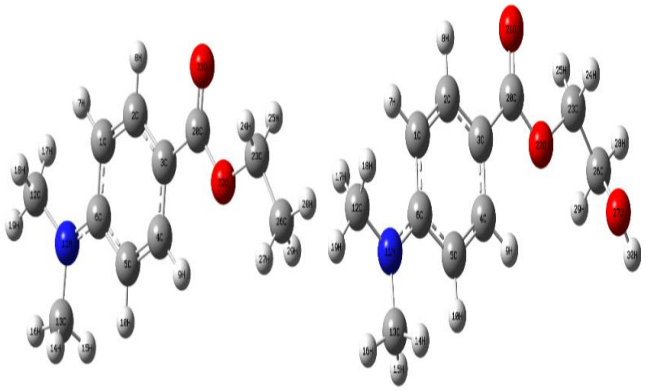

Fig.1. *Optimized molecular structure of compounds 1 and 2*

Table: 1 *Calculated Optimized parameters of compounds 1 and 2*

Bond length (Å)	Calc.		Bond Angle(º)	Calc.	
	1	2		1	2
C_1-C_2	1.382	1.382	C_1-C_2-C_3	121.3	121.3
C_2-C_3	1.399	1.399	C_2-C_3-C_4	118.1	118.2
C_3-C_4	1.399	1.400	C_3-C_4-C_5	121.1	121.0
C_4-C_5	1.384	1.384	C_1-C_2-C_6	120.9	120.8
C_5-C_6	1.415	1.415	C_1-C_5-C_6	117.3	117.4
C_1-C_6	1.416	1.416	C_4-C_5-C_6	121.0	121.0
C_6-N_{11}	1.378	1.378	C_1-C_2-C_7	118.7	118.7
N_{11}-C_{12}	1.454	1.453	C_1-C_6-C_7	120.3	120.3
N_{11}-C_{13}	1.453	1.453	C_1-C_6-N_{11}	121.3	121.2
C_{13}-H_{14}	1.098	1.098	C_6-N_{11}-C_{12}	120.1	120.1
C_3-C_{20}	1.478	1.477	C_2-C_3-C_{20}	118.5	118.7
C_{20}-O_{22}	1.357	1.356	C_3-C_{20}-O_{22}	112.5	112.1

4.2. Natural Bond Orbital Analysis

The distribution of electron density (ED) in various bonding, antibonding orbitals and $E^{(2)}$ energies have been calculated by natural bond orbital (NBO) analysis to give clear evidence of stabilization originating from the hyperconjugation of various intramolecular interaction given in table 2. The natural bond orbital (NBO) analysis was performed using the NBO 3.1 program as implemented at B3LYP/6-311G (d,p) level in order to understand all possible interactions between filled donor and empty acceptor. Table 2 shows some energies of hyperconjugative interaction by second order perturbation theory analysis. The mainly significant interaction in compound 1 is electron donating from the LP_2 O_{21} atom to the antibonding acceptor σ*(C_3-C_{20}), which results in the stabilization energy of 16.54kJ/mol. The other intramolecular hyperconjugative interactions are formed by the orbital overlap between LP_2O_{21}→σ*(C_{20}-O_{22}) and LP_2O_{22}→π*(C_{20}-O_{21}) with larger energies 32.68, 35.64 kJ/mol respectively for compound 2. The larger energy shows the hyperconjugation in compound 1. The bonding concepts such as type of bond orbital, their occupancies, the natural atomic hybrid of which the NBO is composed, the percentage of NBO on each hybrid, and s hybrid label showing the hybrid orbital(sp*) composition (the amount of s-character, p-character) of the compounds 1 and 2. The bonding orbital for both C_1-C_2 and C_1-C_6 with 1.975 and 1.970 electrons have 50% character for C_1 and 50% character for C_2 and has 49% and 51% character for C_1 and C_6. In compound 2 the bonding orbital for σ (C_1-C_2) and σ (C_1-C_6) with 1.975 and 1.970 electrons have 50% and 50% character for C_1 and C_2 and have 49% and 51% character for C_1 and C_6.

Table: 2. *Selected hyperconjugative interactions of compounds 1 and 2*

Compounds	Donor	ED(e)	Acceptor	ED (e)	E^2/kJ/mol
1	O_{21}	1.989 0.031	σ*(C_3-C_{20})	1.52 0.063	16.54
	O_{22}	1.989 0.031	σ*(C_{20}-O_{21})	1.63 0.078	35.65
2	O_{21}	1.989 0.031	σ*(C_{20}-O_{22})	1.48 0.059	32.68
	O_{22}	1.989 0.031	σ*(C_{20}-O_{21})	1.59 0.069	35.64

4.3. Atomic Charge and MESP analysis

Atomic charge calculation has a major role in the application of quantum chemical calculations to molecular system because of atomic charges effect varied properties such as dipole moment, molecular polarizability, electronic structure and acidity–basicity behaviour of compound. Natural charge analysis plot of compounds 1 and 2 is given in Fig.2a. From these results, most of the carbon atoms show negative charge. The oxygen atoms are more electronegative than the carbon atoms, so it is sensible to expect that the oxygen atoms act as electron acceptors and the carbon atoms as electron donors. The C_{20} atom is found to have the highest positive natural charge value of 0.814e. C_{23} atom is very low negatively charged having -0.017e. The charges of oxygen atoms are -0.573e (O_{22} compound 1), -0.565e (O_{22} compound 2). The MESP surface which is a method of mapping electrostatic

potential onto the iso-electron density surface simultaneously displays the molecular shape, size and dipole moments of the molecule, and it provides a visual method to understand the relative polarity [6]. The MESP was mapped with the total density of the molecule for title compound. As can be seen in Fig. 2b, red colour indicates the more electron-rich and blue indicates the electron-poor part.

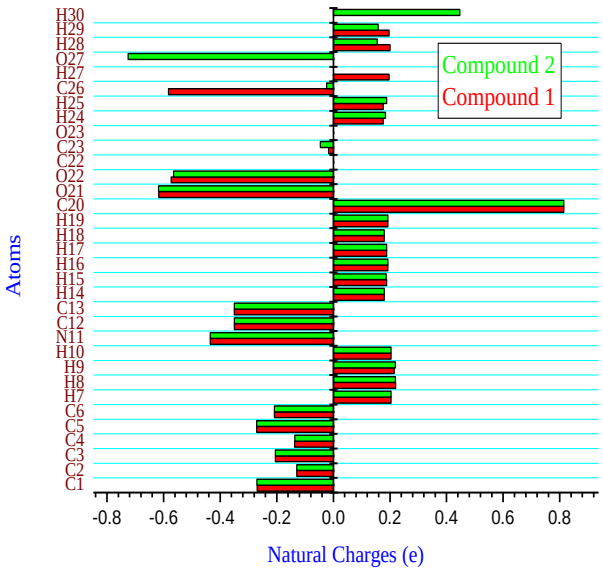

Fig. 2a *Charge distribution plot of compounds 1 and 2*

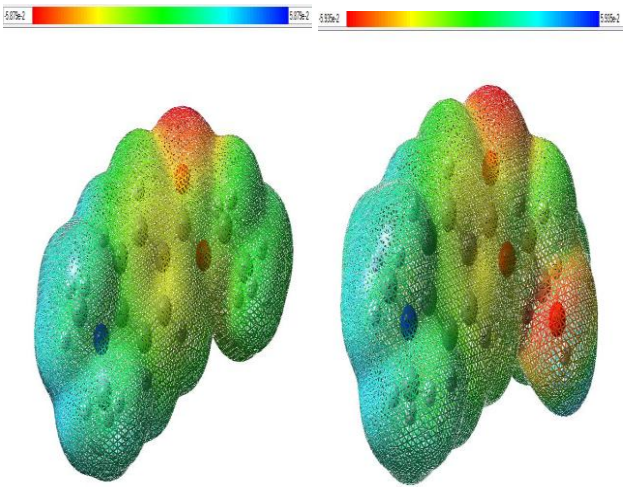

(a) (b)

Fig.2b. *Molecular electrostatic potential mesh map of compound 1 and 2*

4.4. Frontier molecular orbitals analysis

The conjugated molecules are characterized by a small HOMO–LUMO energy separation which is the electronic absorption from the ground state to the first excited state. The figure shows that HOMO is mainly localized on the dimethylamino group, C-O group and the phenyl ring with π bond nature, while LUMO are mainly localized on the dimethylamino group, C-O group and the phenyl ring with π bond nature with σ bond nature. The HOMO-LUMO plot also shows that the electrons transfer from dimethyl amino group to methylene carbonyl group through the phenyl ring (D-π-A) and is evident that there is a possibility of intramolecular charge transformation (ICT). The HOMO, LUMO energy are also calculated and the value of the energy gap between the HOMO and LUMO is 4.523 eV (compound 1), and 4.576 eV (compound 2). The low HOMO-LUMO energy gap shows the intramolecular charge transfer taking place within the molecule. The total (TDOS), partial (PDOS) and overlap population (OPDOS or COOP (Crystal Orbital Overlap Population)) density of states were created to convoluting the molecular orbital information using the Gaussum 3.0 program. The TDOS, PDOS and OPDOS plot of compounds 1 and 2 are plotted in Fig.3. They provide a pictorial representation of MO composition and their contributions to the chemical bonding [7]. The OPDOS show the bonding, anti-bonding and nonbonding nature of the interaction of the two orbitals. The positive value of OPDOS indicates a bonding interaction, negative value means that there is an anti-bonding interaction and zero value shows nonbonding interaction [8].

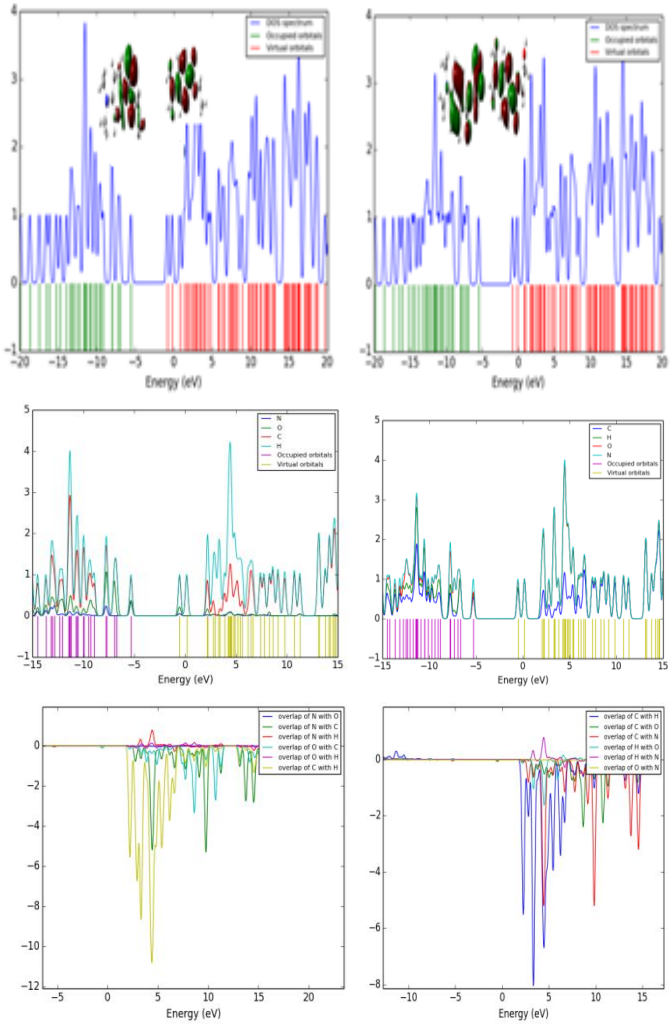

Fig.3 *DOS, PDOS and COOP plot of compounds 1 and 2*

4.5 Dipole moments, Polarizability, first and second order hyperpolarizabily

Quantum-chemical calculations have made an important contribution to the understanding of the molecular NLO processes and the establishment of structure-property relationships [9]. The dipolemoment, polarizabilities and hyperpolarizabilities characterize the response of a system in an applied electric field [10]. The total static dipole moments μ,

the mean polarizabilities $\alpha_{.}$, the anisotropy of the polarizabilities $\Delta\alpha$ and the mean first hyperpolarizabilities β_0 using the x, y and z components are defined as

The total static dipole moments

$$\mu = (\mu_x 2+\mu_y 2+\mu_z 2)^{1/2}$$

The isotropic polarizability is

$$\alpha_0 = \frac{\alpha_{xx} + \alpha_{yy} + \alpha_{zz}}{3}$$

The first order hyperpolarizability (β) was also calculated using the finite-field approach theory. Using the x, y and z components, the magnitude of the first hyperpolarizability tensor can be calculated using the equation is

$$\beta_{tot} = (\beta_x^2 + \beta_y^2 + \beta_z^2)^{1/2}$$

The average second hyperpolarizability equation is

$$[\gamma] = \frac{1}{5}(\gamma_{xxxx} + \gamma_{yyyy} + \gamma_{zzzz} + 2\gamma_{xxyy} + 2\gamma_{xxzz} + 2\gamma_{yyzz})$$

Since the values of the polarizabilities (α) and hyperpolarizability (β) of the Gaussion 09 output are reported in atomic units (a.u) , the calculated values have been converted into electrostatic units (esu) (1 a.u=0.1482 $x10^{-24}$ esu); (1 a.u=8.639 $x10^{-33}$ esu). The B3LYP/6-311G(d,p) level gives the large values of dipole moment, mean polarizability α_0, total polarizabilities, first and second order hyperpolarizabilities. In compounds 1 and 2 the dipole moment values are 1.87 Debye and 1.79 Debye, mean polarizability values are 23.79 x 10^{-24} e.s.u and 21.65 x 10^{-24} e.s.u, and the total polrizability values are 23.50 x 10^{-24} e.s.u and 22.13 x 10^{-24} e.s.u. The first order hyperpolarizability is the measure of the NLO activity of the molecule. The first order hyperpolarizability is 120.73 x 10^{-31} e.s.u and the second order hypepolarizability is 2.61 x 10^{-39} e.s.u for compound 1 respectively.

4.6. Second harmonic generation (SHG) studies

The non-linear optical property of compound 1 was confirmed, and the SHG efficiency in the powdered form was measured obeying the Kurtz and perry powder method [11]. Nd-YAG laser was used as a light source. A fundamental laser beam of 1064 nm wavelength, 8 ns pulse width with 10 Hz pulse rate was made to fall normally on the sample cell. The green light was detected by a photomultiplier tube and displayed on a storage oscilloscope. The SHG relative efficiency of compound 1 was found to be 11 times higher than that of KDP and 47 times higher than that of urea.

4.7 Vibrational Analysis

The vibrational spectral analysis is performed on the basis of the characteristic vibrations of the disubstituted Phenyl ring, dimethyl amino group carbonyl group, methelene and methyl group. The calculated FT-IR and FT-Raman spectra is given in Fig. 4. The theoretical and experimental wavenumbers and the assignments of wavenumbers (Table.3) are discussed below.

Phenyl ring vibration

The numbers of normal vibrations of the substituted phenyl rings are assigned according to Wilson's numbering convention [12] and which is calculated DFT level. The allowed C-H stretching modes of phenyl rings disubstituted is 7b, 2, 20a, 20b and is expected in the region at 3030-3120 cm^{-1}. The observed band in Raman at 3087 cm^{-1} is attributed to mode 7b of phenyl ring (TED 99%). The C-H stretching vibrational modes 2 and 7b appear to be weak, which is due to the hyperconjugation occurs in phenyl ring that induces effective conjugation and charge localization resulting in phenyl ring [13]. C-H in plane bending mode 9a and 9b appeared in the region 1164-1190 cm^{-1}, 1156-1168 cm^{-1} and 18a , 18b are appears in the region 1004-1022 cm^{-1}, 1100-1128 cm^{-1} for the disubstituted benzene. The allowed C-C stretching modes are 8a, 8b, 14, 19a and 19b for the disubstituted benzene derivatives [14].

Dimethyl amino vibrations

The π conjugated path phenyl ring attached with dimethylamino group leads the inter molecular charge transfer interaction of D-π-A type molecules [15]. The C-N stretching is normally observed in the region between 1080-1360 cm^{-1}. In compound 1 (C_6-N_{11}) stretching wavenumber is observed as a weak band in IR and in Raman at 1365 cm^{-1} for the ICT state.

Methelene Vibration

The asymmetric and symmetric CH_2 stretching vibrations normally appear strongly about 2926 and 2853 cm^{-1} [16]. In compound 1 the weak IR band observed at 2978 cm^{-1} and in Raman at 2978 cm^{-1} are due to asymmetric CH_2 stretching.

Carbonyl vibration

The carbonyl group usually observed about 1700-1780 cm^{-1}[17]. The intense band shows the conjugation nature of the carbonyl group. The observed spectrum indicates that the C=O wavenumber is red shift from the usual value. This red shifting wavenumber is due to the intermolecular C-H...O hydrogen bonding with in the molecule.

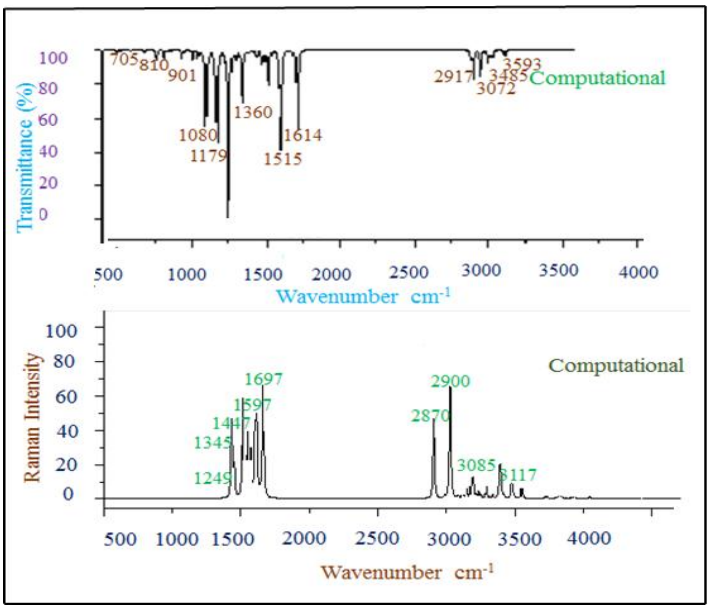

Fig.4 *Computational Spectra of FT-IR and FT-Raman for compound 1*

Table: 3. *Selected vibrational assignments*

Exp		Calc.		Assignments with PED (%)
FT-IR	FT-Raman	1	2	
3208		3113	3112	ν^{R}CH(91)Sym
3087	3087	3096	3096	ν^{R}CH(89)Asym
3062	3051	3032	3034	νCH$_3$(94)
2981	2974	2982	2955	νCH$_2$(79)Asym
2905		2950	2946	νCH$_2$(98)Sym
1695	1690	1710	1711	νC=O(86)
1610	1602	1600	1600	ν^{R}CC(67)Sym
1555	1559	1541	1541	ν^{R}CC(67)Asym
1480		1484	1484	βHCH(65)
1400	1406	1400	1402	βHCC(71)
1367	1365	1355	1343	νCN (51)

4.8 Potential Energy Surface Scan (PES) Analysis

The evaluation of the most stable conformations of compounds 1 and 2 was performed by the potential energy surface (PES) as a function of the dihedral angles that were modified independently at the B3LYP 6-311 G (d,p) level at every 10º for a 360º rotation from 0º around the bond. The conformation of compounds 1 and 2 are related to different rotations, we have determined the conformers by defining orientation are shown in Fig.5. In this kind of rotation occurs, due to the influence of different structural parameters, such as steric, dipolar and hyperconjugative effects including hydrogen bonding interaction [18]. The minimum energy distribution was obtained by choosing the dihedral angles C_1-C_6-N_{11}-C_{12}, C_1-C_6-N_{11}-C_{13}, C_6-N_{11}-C_{12}-H_{14}, C_6-N_{11}-C_{12}-H_{17} and C_3-C_{20}-O_{22}-C_{23} are compound 1. This dihedral angle was the relevant coordinate for conformational flexibility within the molecule. In compound 1, the lowest global minimum energy was obtained at 0º, 180º and 360º in the potential energy curve with an energy value -633.585kJ/mol, which is due to the possibility of strong C_5-H_{10}…N_{11} hyper conjugation with the interatomic distance H_{10}…N_{11} (2.121Å) which leads to the NLO active site (N_{11}) as supported by structural, vibrational and NBO analysis. The maximum energy was obtained at 90º and 270º with the energy value -633.565 kJ/mol. High barriers was noticed as 20kJ/mol due to the influence of hyperconjugative interaction.

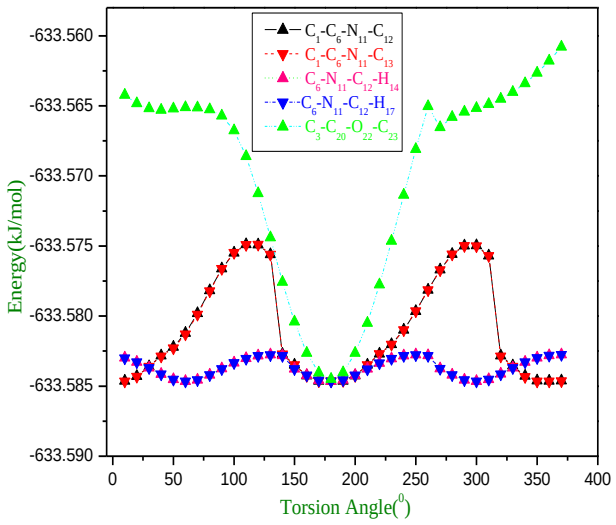

Fig.5*. Potential energy surface scan curve of compound 1*

5. CONCLUSION

The complete molecular structure, vibrational spectra and non-linear properties of (compound 1) and (compound 2) have been performed based on the DFT calculations at B3LYP/6-311G(d,p) level analyzed and compared with the experimental values. The NBO analysis explains the presence of π electron cloud movement and hyperconjugative interaction. The low HOMO-LUMO energy gap explains the intramolecular charge transfer taking place within the molecule. The calculated hyperpolarizability and SHG measurement of compound 1 shows the NLO activity.

REFERENCES

[1] Contreras, P. P.; Tyagi, P.; Agarwal, S. Low volume shrinkage of polymers by photopolymerization of 1,1-bis(ethoxycarbonyl)-2-vinylcyclopropanes. *Polym. Chem. 6* (12), 2297-2304, **(2015).**

[2] R.Denningten, T. Keith, J. Millam, Gaussview version 5.0.8, Gaussian, Inc, 235 wallingford CT, **(2009)**.

[3] E.D. Glendening, J.K. Badenhoop, A.E. Reed, J.E. Carpenter, J.A. Bohmann, C.M. Morales, F. Weinhold, NBO 5.0, Theoretical Chemistry Institute, University of Wisconsin, Madison, **(2001).**

[4] A. Domenicano, A. Vaciago, C.A. Coulson, Acta Crystallogr. Sect.B 31, 1630 **(1975).**

[5] H.W. Thomson, P. Torkington, J. Chem. Soc. 171 640 **(1945).**

[6] I. Fleming, Frontier Orbitals and Organic Chemical Reactions, John Wiley and Sons, New York, (**1976).**

[7] M. Chen, U.V. Waghmare, C.M. Friend, E. Kaxiras, A density functional study of clean and hydrogen-covered α-MoO3(010):Electronic structure and surface relaxation, Journal of Chemical Physics, **109** 6854-6860 **(1998).**

[8] M.Chen, U.V.Waghmare, C.M. Friend, E. Kaxiras, J. Chem. Phys. **109** 6854-6860 **(1998).**

[9] F. Meyers, S.R. Marder, B.M. Pierce, J.L. Brédas, J. Am. Ceram. Soc. 116 110703 **(1994).**

[10] C.R. Zhang, H.S. Chem, G.H. Wang, Chem. Res. Chin. Uni. 20, 640 **(2004).**

[11] S.K. Kurtz, T.T. Perry, J. Appl. Phys 39, 3798 **(1968).**

[12] G. Varsanyi, Vibrational Spectra of Benzene Derivatives, Academic Press, New York, (**1969).**

[13] Pinaky Sett, Shirsendu Datta and Prabal Kumar Mallick, J. Raman spectrosc. 42, 859 **(2011).**

[14] F. R. Dollish, W. G. Fateley and F. Bentley, Characteristic Raman Frequencies of Organic Compounds. Wiley, Chichester, (**1974).**

[15] A.M. Brouwer, R.J. Wilbrandt, Chem. Phys. Chem. 100 9678 **(1996).**

[16] N. P. G. Roeges, A Guide to the Complete Interpretation of Infrared spectra of Organic Structure; Wiley: New York, (**1999).**

[17] Toshikuni Kaino, J. Opt. A: Pure Appl. Opt. 2 **(2000).**

[18] J.B.Bhagyasree, H.T.Varghese, C.Y.Panicker, J.Samuel, C.Van Alsenoy, K.Bolelli, I.Yildiz, E.Aki, Spectrochim. Acta **102** 99 **(2013).**